Raman spectroscopic study of Na1/2Bi1/2TiO3-x%BaTiO3 single crystals as a function of temperature and composition

Liang Luo, Wenwei Ge, Jiefang Li, D. Viehland, Charles Farley, Robert Bodnar, Qinhui Zhang, and Haosu Luo

Raman spectroscopic study of $Na_{1/2}Bi_{1/2}TiO_3$-x%$BaTiO_3$ single crystals as a function of temperature and composition

Liang Luo,[1] Wenwei Ge,[1,a)] Jiefang Li,[1] D. Viehland,[1] Charles Farley,[2] Robert Bodnar,[2] Qinhui Zhang,[3] and Haosu Luo[3]

[1]*Department of Materials Science and Engineering, Virginia Tech, Blacksburg, Virginia 24061, USA*
[2]*Department of Geosciences, Virginia Tech, Blacksburg, Virginia 24061, USA*
[3]*Shanghai Institute of Ceramics, Chinese Academy of Sciences, 215 Chengbei Road, Jiading, Shanghai 201800, China*

A Raman spectroscopic study of $Na_{1/2}Bi_{1/2}TiO_3$-x%$BaTiO_3$ (NBT-x%BT) single crystals with $x = 0$ and 5.6 has been performed as a function of temperature from 25 to $600\,°C$. The general features of the Raman spectra for the various compositions were similar over the region of the phase diagram investigated, with only subtle changes between rhombohedral (R), tetragonal (T) and cubic phases. The peaks were broad, with no significant narrowing on cooling through a phase transition. We find evidence of an oxygen octahedral rotational mode in the paraelectric state. On cooling near and below the ferroelectric Curie temperature, a gradual change in intensity of the A-O and B-O peaks occurred with decreasing temperature. Evidence of a ferroelectric → antiferroelectric transition was found near $200–250\,°C$, consistent with the onset of dispersion in the dielectric constant. The phase transition mechanism was discussed. The findings indicate the presence of a broad distribution of quasistatic local structural distortions, which only have subtle differences in the various average structures. © *2011 American Institute of Physics*. [doi:10.1063/1.3587236]

I. INTRODUCTION

The crystal structure of $Na_{1/2}Bi_{1/2}TiO_3$-x%$BaTiO_3$ (or NBT-x%BT) is sensitive to modest changes in x as x%$BaTiO_3$ (BT) increases. The phase diagram (Fig. 1) shows that a high temperature tetragonal (T) ferroelastic phase is suppressed[1] for $x < 4$, and a morphotropic phase boundary (MPB) between ferroelectric rhombohedral (R) and T phases occurs near $x = 6$.[2] Structural investigations[3] of $NBT − 5.6\%BT$ crystals have revealed a ferroelectric R phase in the zero-field-cooled (ZFC) condition, but a ferroelectric T phase in the poled condition, indicating a history dependent phase stability in the vicinity of the MPB. For these MPB compositions, longitudinal piezoelectric d_{33} coefficients as high as 500 pC/N have been reported in poled (001) crystals.[4] Interestingly, the value of d_{33} was highest in the ferroelectric T phase side of the MPB, rather than the R phase, as is observed for Pb-based MPB crystals[5,6] where low symmetry structurally bridging phases are known to be present.[7–10]

The temperature dependent phase transformation characteristics of NBT-x%BT, such as the dielectric constant, are known to be diffuse.[2] In the ferroelectric R phase field, the dielectric response is known to be frequency dispersive,[11] similar to relaxor ferroelectrics. Relaxors are characterized by the presence of a local polarization to temperatures much higher than the temperature of the dielectric maximum (T_{max}), as evidenced by deviations from linear temperature dependent optical constants,[12] linear thermal expansion[13] and linear Curie-Weiss behavior.[14] However, investigations of the thermal expansion and Curie-Weiss behavior of NBT-x%BT[15] failed to reveal the presence of a local polarization to high temperatures. Rather, these properties have been found to be linearly dependent on temperature above T_{max}. In fact, in the temperature range near T_{max}, various intermediate ferroelectric and antiferroelectric phases have previously been reported, sandwiched between cubic and R phase fields. For example, neutron scattering and high-resolution synchrotron x-ray diffraction (XRD) identified a relatively wide transition range over which T and R phases coexist,[16–18] and transmission electron microscopy (TEM) images of powder samples evidenced an intermediate modulated orthorhombic (O) phase between the R and T phases in the temperature range between 230 and $300\,°C$.[19,20]

Raman spectroscopy represents another local probe to study NBT-x%BT.[21,22] Theoretically, for the ferroelectric rhombohedral R3c phase of NBT-x%BT, there are 13 Raman active modes,[23] including $7A_1$ and 6E modes. Prior experimental investigations have shown that these peaks are broad and cannot all be resolved from each other but can be categorized into those pertaining to one of three frequency ranges.[21,22] These are: (1) a low wavenumber range of $100–200\ cm^{-1}$ which is believed to be related to Na-O vibrations; (2) a mid wavenumber range of $200–400\ cm^{-1}$ which is believed to be related to Ti-O vibrations; and (3) a high wavenumber range of $400–800\ cm^{-1}$ which is believed to be related to oxygen octahedral vibrations and rotations. The cubic phase should not have any first order Raman modes.[24,25] However, local static distortions have been shown by Uwe *et al.*[26] to yield second order Raman-bands. Such effects of local distortions also lead to line broadening.
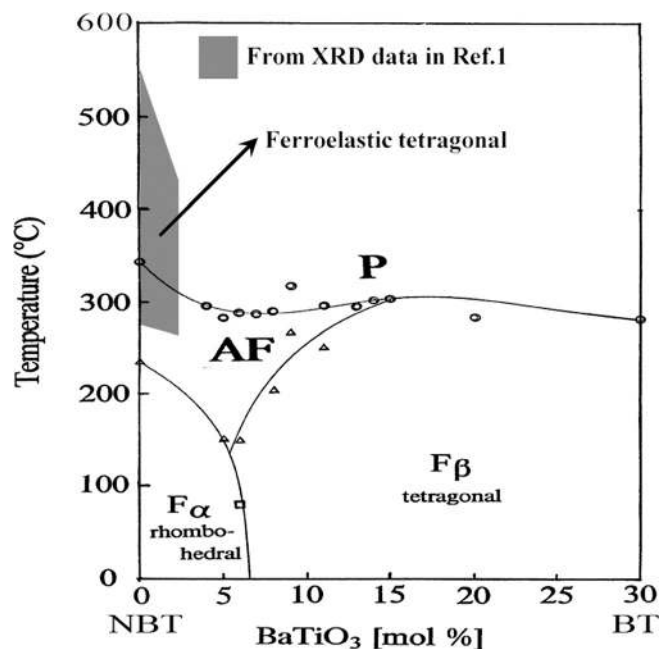
a)Electronic mail: wenweige@vt.edu.

FIG. 1. Phase diagram of $(Na_{1/2}Bi_{1/2})TiO_3$-$BaTiO_3$ (NBT-BT) solid solution (F_α: Ferroelectric rhombohedral phase, F_β: Ferroelectric tetragonal phase, AF: Antiferroelectric phase, P: Paraelectric phase Reprinted with permission from ref. 2. Copyright [1991], APEX/JJAP.).[2]

Temperature dependent studies of local distortions in relaxor ferroelectrics have previously been performed by Raman spectroscopy, revealing second order Raman effects in the cubic phase over a broad temperature range,[27,28] extending to the Burn's temperature[12] at which point deviations from linearity in the Curie-Weiss behavior being to occur on cooling. Raman studies of NBT as a function of temperature[21,29] and pressure[25] have been reported. However, systematic studies of Raman scattering for NBT-x%BT have not been performed as a function of temperature over the compositional range were notable changes in phase stability occur with modest changes in x%BT (see Fig. 1). Such an investigation could provide important information concerning the presence of local distortions in NBT-x%BT, and the manner in which the average crystal structure is affected by changes in local distortions. Here, we present such an investigation for NBT-x%BT single crystals.

II. EXPERIMENTAL PROCEDURE

Single crystals of NBT and NBT-x%BT were grown by a top-seeded solution growth (TSSG) method.[30] The concentrations of Ba ions in the as-grown condition were determined by inductive coupled plasma atomic emission spectrometry (ICP-AES) to be 5.6at%. $[001]_p$ (subscript p refers to pseudocubic perovskite axes) oriented wafers of NBT and NBT-5.6%BT single crystals were cut into $5 \times 5 \times 0.3$ mm plates, and the surfaces were polished to 0.3 μm. Raman spectra were obtained using a JY Horiba Lab-Ram HR (high resolution) design with an 800 mm spectrograph that was equipped with a 100 mW, air-cooled 514 nm Argon laser for excitation; an air-cooled ($-70\,°C$) CCD detector with a 1024×256 pixels front illuminated chip; 2400 and 600 grooves/mm gratings; confocal optics; an internal Ne source for wavelength calibration; an FTIR module that
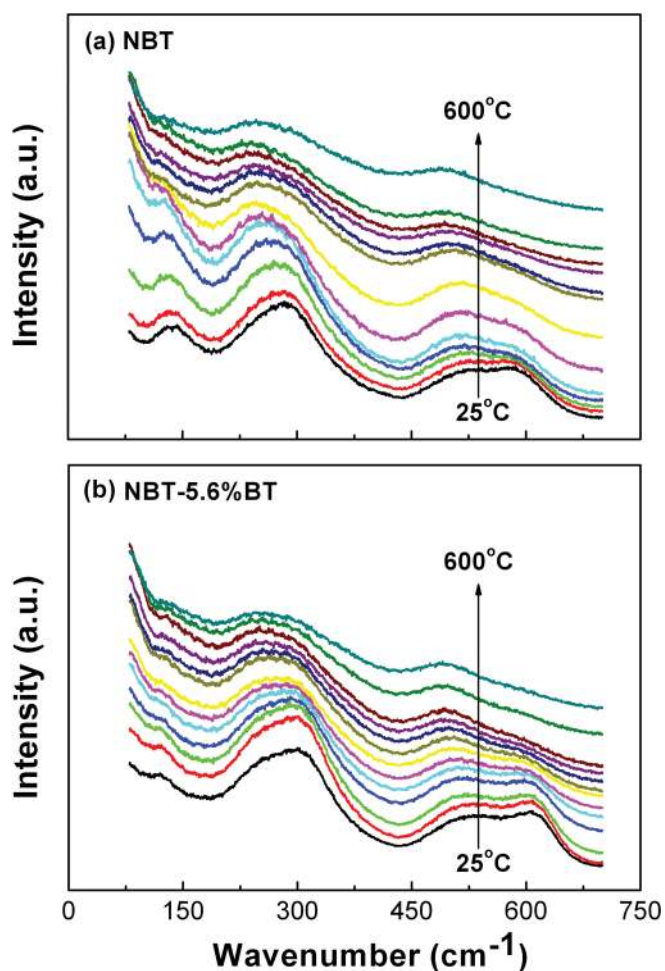

FIG. 2. (Color online) Temperature-dependent Raman spectra of (a) NBT and (b) NBT-5.6%BT from 25 °C to 600 °C.

permits FTIR and Raman analysis of the same spot without moving the sample. The microprobe was equipped with an Olympus microscope with a range of objective lenses and filters, and with a Linkam THMS600 heating/cooling stage.

III. RESULTS

Figure 2 shows the temperature dependent spectra collected at 25 °C and 50 °C, and at 50 °C steps thereafter up to 600 °C for (a) NBT and (b) NBT-5.6%BT. To simplify this presentation of data, we show Raman spectra for [(a) and (c)] NBT and [(b) and (d)] NBT-5.6%BT measured at 25 °C (left column) and 600 °C (right column) in Fig. 3. In order to better illustrate changes in peak characteristics with x%BT and temperature, spectral deconvolution to Lorentzian and Gaussian-shaped peaks is shown in Fig. 3. First, we note that the spectral characteristics of the peak deconvolution for NBT at room temperature [Fig. 3(a)] are nearly identical to those previously reported by Kriesl *et al.*[23,31] We observed one intense peak near 135 cm^{-1} previously assigned to Na-O lattice vibrations,[23,25] one dominant peak near 275 cm^{-1} previously assigned to Ti-O vibrations,[21,25] and three peaks in the range of 400–600 cm^{-1} previously assigned to oxygen octahedral vibrations/rotations (designated as C′, C″, and C‴).[21,24,25,32,33] The relative intensity of C‴ is larger than
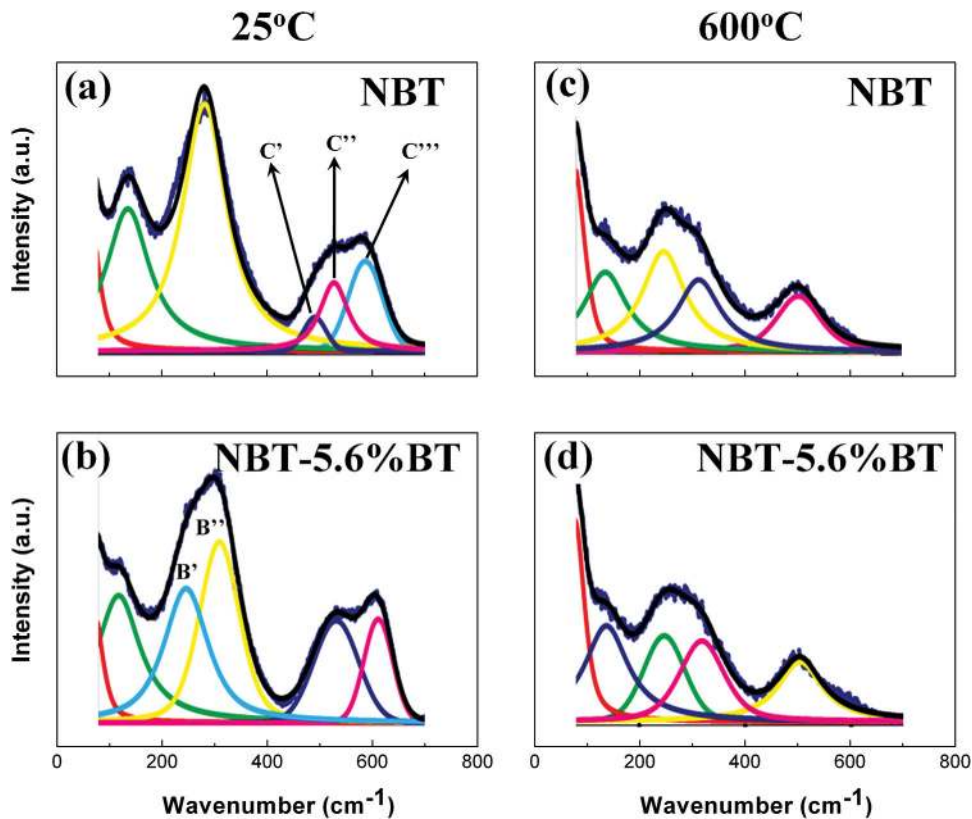
FIG. 3. (Color online) Raman spectra of [(a) and (c)] $(Na_{1/2}Bi_{1/2})TiO_3$ (NBT) and [(b) and (d)] NBT-5.6%BT at 25 °C (left column) and 600 °C (right column) and the spectra deconvolution.

that of C'' in NBT crystal and was further increased by 5.6% BT doping, whereas it was the opposite in NBT and NBT-11%BT powder samples at ambient condition.[31] Second, with the addition of $x = 5.6$%BT to NBT [Fig. 3(b)], two changes were observed: (1) the peak at 275 cm^{-1} split into two peaks, designated as B' and B''; and (2) the peak C' in the high frequency range disappeared, and C'' and C''' became dominant.

Next, we deconvoluted the peaks in Figs. 3(c) and 3(d) collected at 600 °C. All peaks were notably decreased in relative intensity on heating to 600 °C, and the spectra for the various compositions were all similar to each other at this temperature. Several other qualitative changes in the features of the Raman spectra can be discerned with this change in temperature, specifically: (1) for all crystals, the high frequency C peaks merged into a single peak; and (2) for NBT, the mid-range B peak split, becoming similar to that for NBT-5.6%BT. The merging of the C peaks at 600 °C is somewhat similar to that previously reported by Kriesel *et al.*[25] with increasing pressure (ΔP), except for the fact that in our experiments the three peaks merged toward C', rather than toward C'' as observed with ΔP. Kriesel *et al.*[25] attributed the observed spectral changes to the overlapping of A_1 and E bands, and to the loss of longitudinal (LO) and transverse (TO) character, rather than to a T→C transition. Their reasoning is seemingly correct for the case of ΔP, in particular since their C peak became notably more intense with increasing ΔP. However, recent XRD studies have shown that the average crystal structure of NBT at 600 °C is cubic.[1] This, in addition to the fact that our C Raman peaks intensity became notably weaker with increasing temperature, strongly suggests that scattering is second order. It is inter-

esting to note in Fig. 2 that the changes in the C peak(s) with increasing temperature between 25 and 600 °C were qualitatively similar for NBT and NBT-5.6%BT. This is important to note because the average crystal structure of NBT is (paraelectric) tetragonal between 300 and 540 °C,[34] whereas that of NBT-5.6%BT appears to be cubic by XRD[1] above 300 °C. This suggests that oxygen rotations are present in both the high temperature tetragonal and cubic phases, which have short correlation lengths.

The splitting of the B peak(s) at room temperature with increasing x for NBT-x%BT reveals a change in symmetry (relative to NBT), to a structure whose irreducible representation has a higher number of Raman active modes. It is noteworthy, due to the proximity of the MPB for NBT-5.6%BT, that the R phase (R3c) has 13 Raman-active modes whereas the T phase (P4bm) has 15.[23] With increasing temperature to 600 °C, deconvolution of the spectra revealed that the B peak splitting persisted for NBT-5.6%BT far above T_{max} in the cubic phase. Furthermore, for NBT, the single B peak in the R phase was found to split with increasing temperature to T_{max}, in a manner identical to that for NBT-5.6%BT. These results show that similar polar active Ti-O lattice vibrations persist in the paraelectric state of both NBT and NBT-5.6%BT, independent of whether the average structure is tetragonal ($x = 0$) or cubic ($x = 5.6$%).

Figure 4 shows a summary of the band frequencies as a function of temperature for NBT. We can identify two phase transition temperatures based on changes in the band frequencies. The first occurs at 250 °C on cooling, where $C'' + C''' → C' + C'' + C'''$ and $B' + B'' → B''$. Please note that this temperature corresponds to the onset of dielectric dispersion. The observed changes in the band frequencies
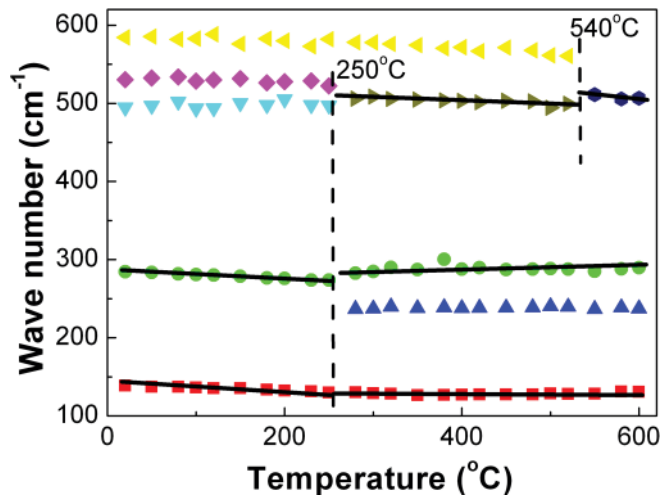
FIG. 4. (Color online) Peak position as a function of temperature of NBT.

FIG. 5. Integrated Intensity of the B-O peaks of (a) NBT and (b) NBT-5.6%BT as a function of temperature.

demonstrate that a change in symmetry does indeed occur at a second transformation temperature below that of T_{max}. Above this temperature, the Raman peak splitting of NBT is similar to those of NBT-5.6%BT (see Fig. 3): i.e., the symmetries are identical above 250 °C. The principle difference between the ferroelectric R and T phases was that the polarization in the T phase formed without a change in peak splitting below 250 °C, whereas that in the R phase exhibited the changes mentioned above.

Figure 5 the 285 cm^{-1} (B-O) peak as a function of temperature for (a) NBT and (b) NBT-5.6%BT. This particular phonon peak has been reported to be directly involved in the ferroelectric structural phase transformation.[35] A negative temperature dependence of the mode was previously cited as evidence of soft-mode behavior, where the Ti-O displacements in the oxygen octahedral become more symmetric above the ferroelectric Curie temperature.[35] In Fig. 5, where applicable, we have marked the temperature of the dielectric maximum (T_{max}), temperature of the onset of dielectric dispersion, and the temperature of the high temperature cubic $\rightarrow$ paraelectric tetragonal transition. Inspection of Fig. 5 reveals slow and gradual changes in the peak intensities over a temperature range of 300 to 600 °C for all samples studied. Notable peak intensity is observed to temperatures far above T_{max}, and even further above the T $\rightarrow$cubic transition for NBT near 600 °C. In the ferroelectric phase below about 200 °C, the intensity exhibited a plateau and became nearly constant on further cooling. Please note that all compositions studied exhibited a similar temperature dependence for their 285 cm^{-1} mode. However, for NBT-5.6%BT, we note a difference in the B' (240 cm^{-1}) peak relative to the B'' peak (285 cm^{-1}). Interestingly, the intensity of the B' peak was notably weaker and less temperature dependent compared to the B'' peak. In fact, its intensity was nearly constant over the temperature range of 200 to 600 °C. Only in the ferroelectric tetragonal phase did the B' intensity begin to increase, and then only modestly.

The integrated intensity for the 135 cm^{-1} peak as a function of temperature is shown in Fig. 6 for NBT. The 135 cm^{-1} peak shows a strong increase in intensity on cooling
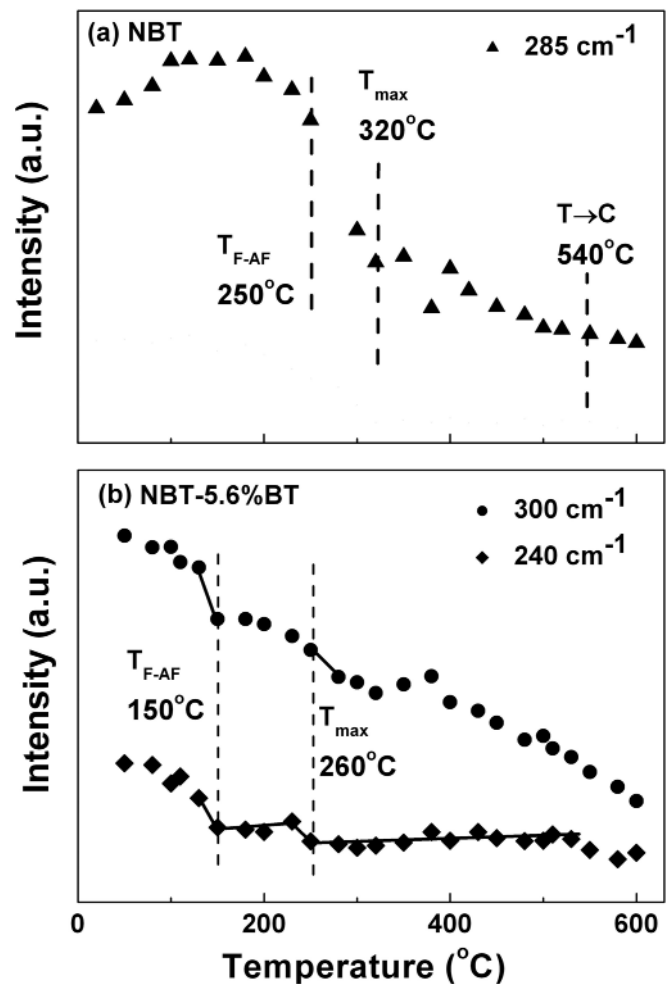
between T_{max} and the second transition where dielectric dispersion begins to become evident. At temperatures above T_{max}, the intensity of the 135 cm^{-1} peak is very low. The 135 cm^{-1} peak is associated with Na-O vibrations, and these
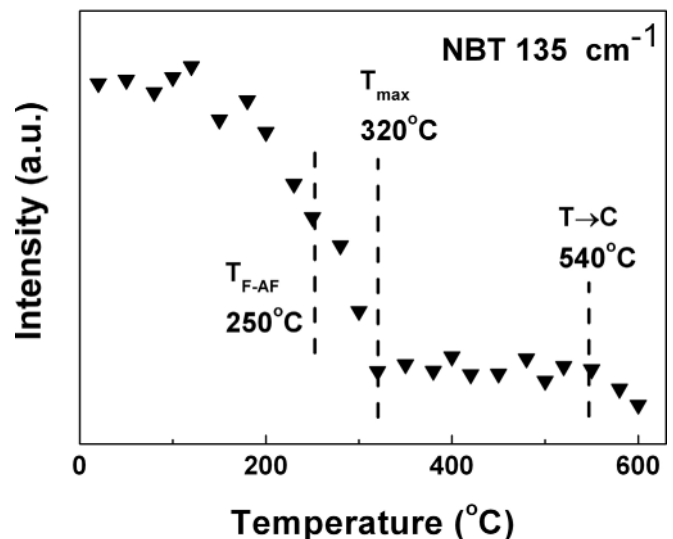

FIG. 6. Integrated Intensity of the A-O peaks of NBT as a function of temperature.

results indicate that Na-O displacements in the oxygen octahedral become very symmetric above T_{max}.

IV. DISCUSSION AND SUMMARY

First, we note that all the line widths of all the peaks of all compositions at all temperatures studied were very broad. There was little sharpening of peaks at a phase transition temperature, nor were there any significant changes with compositional modification. Thus, the general features of the lattice vibrations are similar in the cubic, R, and T phase regions. Only subtle differences were revealed by deconvolution of the spectra by combination of Lorentzian and Gaussian peak fittings. The broadness of the peaks indicates the presence of quenched disorder, where the widths of the line are related to dispersion in the vibrational modes. Second, Raman active peaks were observed to persist into the high temperature cubic phase above 600 °C. This is far above T_{max} of both NBT and NBT-5.6%BT.

The B-O vibrations near 285 cm^{-1} are believed to be related to the ferroelectric phase transformation and soft mode.[35] The intensity of this peak was found to slowly decay with increasing temperature between 200 and 600 °C, with notable intensity remaining at 600 °C. Similar results were found for NBT and NBT-5.6%BT. These results reveal the presence of local polar distortions above the temperature of the dielectric maximum. We attempted to analyze these local distortions following the approach of El Marssi *et al.*,[36] who demonstrated for relaxor ferroelectrics that the inverse of the Raman intensity divided by the temperature (I/T_K) deviated from Curie-Weiss behavior beginning near the Burn's temperature where the onset of local polarization has been observed by dielectric and optical indicatrix data.[12,14] Their approach was based on the assumption that the radius of the polarization did not vary much with temperature, and thus the Raman intensity reflected the behavior of the static dielectric susceptibility. However, for our NBT-x%BT crystals, plots of I/T_K for the 285 cm^{-1} (B″) peak did not reveal any region of linear behavior up to at least 600 °C (data not shown), which was 300 °C above T_{max}. Thus, we can infer that any local polar distortions in the high temperature phase of NBT-x%BT are different in nature from those of relaxor ferroelectrics, lacking spatial and temporal correlations that are preserved with decreasing temperature. Please note that similar observations were made for NBT (in the paraelectric tetragonal phase) and NBT-x%BT (in the paralelectric cubic phase), i.e., they are independent of the symmetry of the high temperature paraelectric state.

Evidence of local polarization in the high temperature phase can be found by comparing the difference in the temperature dependence of the intensity for the B′ and B″ peaks. Please note that this peak splitting was common to both NBT and NBT-5.6%BT for temperatures above 250 °C but remained present at lower temperatures only for NBT-5.6%BT in its tetragonal ferroelectric phase. Comparisons of the 240 cm^{-1} (B′) and 285 cm^{-1} (B″) peaks for NBT-5.6%BT [see Fig. 5(c)] reveal notably different behaviors. In particular, the intensity of the B′ peak was much lower and temperature independent above 260 °C. With increasing tem-

perature to near 600 °C, the intensity of the B″ peak gradually decayed to that of B′. Only on cooling in the ferroelectric tetragonal phase region for NBT-5.6%BT did the B′ peak intensity began to gradually increase with decreasing temperature. These results indicate a unique anisotropic behavior of local polarization in the high temperature paraelectric phase for both NBT and NBT-5.6%BT.

The temperature dependence of the intensity of the 135 cm^{-1} peak for the A-O vibrations provides further insight into the evolution of local polarization with temperature. Please note in Fig. 6 that the intensity of the 135 cm^{-1} peak was nearly zero above T_{max}, and only below this temperature did the intensity increase. Comparisons of the results in Figs. 5 and 6 thus reveal a difference between the A-O and B-O displacements with increasing temperature. Below T_{max}, Na-O and Bi-O displacements may contribute to the dipole moment, but not above. However, significant Ti-O displacements clearly persist in the high temperature cubic state.

Based on the negative frequency shift of bands A and B with increasing pressure, Kreisel *et al.*[25] proposed a two-step phase-transition mechanism from relaxor ferroelectric R to antiferroelectric orthorhombic (Pnma) for NBT. These are (1) from R to intermediate antiferroelectric phase I by A-cation displacements from parallel $[111]_p$ to antiparallel $[100]_p$, companying restoring of the Ti-cations from parallel $[111]_p$ displacements to the center of oxygen octahedral at 2.8 GPa; and (2) from a$^-$ a$^-$ a$^-$ to a$^-$ b$^+$ a$^-$ octahedral tilt systems at 5 GPa. These same trends for bands A and B can be seen with increasing temperature in Fig. 4, as previously reported for increasing pressure.[25] This suggests that the phase-transition mechanism for NBT with increasing temperature is similar to that just mentioned above with increasing pressure. The transition temperature of 250 °C in Fig. 4 indicates that the ferroelectric→antiferroelectric transition corresponds to the onset of dielectric dispersion: please note that antiferroelectriclike double P-E loops have also been reported near this onset.[37] Recently, TEM studies by Dorcet *et al.*[19] revealed a modulated orthorhombic (Pnma) phase between 230 °C and 300 °C in NBT. This orthorhombic (Pnma) phase was an intermediate phase, which transformed to a tetragonal one with increasing temperature. Our Raman data are consistent with these temperature dependent TEM results, although it was difficult to identify all the splitting of the B band of this intermediate phase. Two fold splitting of band B was observed above 250 °C, as can be seen in Fig. 4; however, more complex splitting of the B band was found at room temperature with increasing pressure.[25] After substituting 5.6%BT into NBT, the B band split into B′ (240 cm^{-1}) and B″ (285 cm^{-1}) at room temperature. The relative intensity and temperature dependence of B″ for NBT-5.6%BT was similar to that of B for NBT, but the relative intensity of B′ was much lower than that of B″ and nearly temperature independent above 150 °C. These results reveal that Ba modification increases the orthorhombic or tetragonal distortion in NBT by favoring $[100]_p$ or $[001]_p$ Ti-cation displacements.

We summarize our observations with respect to the phase diagram of NBT-x%BT, given in Fig. 1. In the high

temperature paraelectric phase, whether T (x = 0) or cubic (x = 5.6%), asymmetric T-O vibrations result in a local polarization. The correlation radius of the local polarization and time correlations between clusters may depend notably on temperature, unlike that for relaxor ferroelectrics.[38] These polarization fluctuations gradually increase with decreasing temperature on approaching the dielectric maximum. The dielectric maximum and transition to the ferroelectric phases is characterized by the onset of asymmetric A-O vibrations. Comparison of the temperature dependence of the A-O and B-O vibration modes suggests that there are two complimentary contributions to the formation of a stable ferroelectric polarization below T_{max}, both for the R (x = 0) and T (x = 5.6) ferroelectric phases.

The only differences between the R and T ferroelectric phases are (1) the loss of the 240 cm^{-1} Ti-O mode in the R phase; and (2) a triplet splitting of the oxygen octahedral vibration modes (C', C'', and C''') in the R phase, relative to a doublet splitting (C'' and C''') in the T. The triplet splitting is consistent with the R-type octahedral rotations[39,40] which occur at the $q = (111)\pi/a$ point of the Brillouin zone. This represents opposite octahedral rotations in successive layers. The doublet splitting is consistent with the M-type octahedral rotations[39,40] which occur at the $q = (110)\pi/a$ point of the Brillouin zone. This represents the same sense of rotation in successive layers. Both of these modes involve oxygen rotations that are nonpolar and that occur along the $[001]_p$. We believe that the transformation to the R-type rotational mode may be key to the stabilization of the R ferroelectric phase. Rotostrictive couplings of the polarization to the R-type oxygen rotations are known,[41] which have been shown to be important to ferroelectric phase stability.[42]

In summary, a Raman spectroscopic study of NBT-x%BT single crystals for x = 0 and 5.6 has been performed as a function of temperature. The results indicate the presence of a broad distribution of local structural distortions, which only have subtle differences between the various average structures found in the NBT-x%BT phase diagram. Our findings demonstrate the presence of a local polarization due to asymmetric Ti-O vibrations up to temperatures much higher than T_{max}, whose time and spatial correlations change notably with temperature. Below T_{max}, we find the onset of asymmetric Na-O vibrations, and the beginnings of the stability ranges of the T and R ferroelectric phases. Evidence indicates that the relative stability of the T and R ferroelectric phases is in part determined by differences in oxygen octahedral rotations.

ACKNOWLEDGMENTS

[1]W. Ge, H. Cao, C. DeVreugd, J. Li, D. Viehland, Q. Zhang, and H. Luo, "Influence of BaTiO$_3$ Content on the Structure and Properties of Na$_{0.5}$Bi$_{0.5}$TiO$_3$ Crystals," J. Am. Ceram. Soc.

[2]T. Takenaka, K. Maruyama, and K. Sakata, Jpn. J. Appl. Phys. **30**, 2236 (1991).

[3]W. W. Ge, H. Cao, J. F. Li, D. Viehland, Q. H. Zhang, and H. S. Luo, Appl. Phys. Lett. **95**, 162903 (2009).

[4]Q. H. Zhang, Y. Y. Zhang, F. F. Wang, Y. J. Wang, D. Lin, X. Y. Zhao, H. S. Luo, W. W. Ge, and D. Viehland, Appl. Phys. Lett. **95**, 102904 (2009).

[5]S. E. Park and T. R. Shrout, J. Appl. Phys. **82**, 1804 (1997).

[6]Y. P. Guo, H. S. Luo, D. Ling, H. Q. Xu, T. H. He, and Z. W. Yin, J. Phys. Condens. Matter **15**, L77 (2003).

[7]D. La-Orauttapong, B. Noheda, Z. G. Ye, P. M. Gehring, J. Toulouse, D. E. Cox, and G. Shirane, Phys. Rev. B **65**, 144101 (2002).

[8]Z. G. Ye, B. Noheda, M. Dong, D. Cox, and G. Shirane, Phys. Rev. B **64**, 184114 (2001).

[9]B. Noheda, D. E. Cox, G. Shirane, J. Gao, and Z. G. Ye, Phys. Rev. B **66**, 054104 (2002).

[10]H. Cao, J. F. Li, D. Viehland, and G. Y. Xu, Phys. Rev. B **73**, 184110 (2006).

[11]V. Isupov, Ferroelectrics **315**, 123 (2005).

[12]G. Burns and F. H. Dacol, Solid State Commun. **48**, 853 (1983).

[13]A. S. Bhalla, R. Guo, L. E. Cross, G. Burns, F. H. Dacol, and R. R. Neurgaonkar, Phys. Rev. B **36**, 2030 (1987).

[14]D. Viehland, S. J. Jang, L. E. Cross, and M. Wuttig, Phys. Rev. B **46**, 8003 (1992).

[15]I. P. Pronin, P. P. Syrnikov, V. A. Isupov, V. M. Egorov, and N. V. Zaitseva, Ferroelectrics **25**, 395 (1980).

[16]G. O. Jones and P. A. Thomas, Acta Crystallogr. Sec. B **56**, 426 (2000).

[17]J. Suchanicz and J. Kwapulinski, Ferroelectrics **165**, 249 (1995).

[18]J. Suchanicz, Ferroelectrics **200**, 319 (1997).

[19]V. Dorcet, G. Trolliard, and P. Boullay, Chem. Mater. **20**, 5061 (2008).

[20]G. Trolliard and V. Dorcet, Chem. Mater. **20**, 5074 (2008).

[21]M. S. Zhang and J. F. Scott, Phys. Rev. B **34**, 1880 (1986).

[22]I. G. Sinii, T. A. Smirnova, and T. V. Kruzina, Fiz. Tverd. Tela **33**, 110 (1991).

[23]J. Kreisel, A. M. Glazer, G. Jones, P. A. Thomas, L. Abello, and G. Lucazeau, J. Phys. Condens. Matter **12**, 3267 (2000).

[24]U. D. Venkateswaran, V. M. Naik, and R. Naik, Phys. Rev. B **58**, 14256 (1998).

[25]J. Kreisel, A. Glazer, P. Bouvier, and G. Lucazeau, Phys. Rev. B **63**, 174106 (2001).

[26]H. Uwe, K. B. Lyons, H. L. Carter, and P. A. Fleury, Phys. Rev. B **33**, 6436 (1986).

[27]J. Toulouse, F. Jiang, O. Svitelskiy, W. Chen, and Z. G. Ye, Phys. Rev. B **72**, 184106 (2005).

[28]A. Slodczyk, P. Daniel, and A. Kania, Phys. Rev. B **77**, 184114 (2008).

[29]I. G. Siny, T. A. Smirnova, and T. V. Kruzina, Ferroelectrics **124**, 207 (1991).

[30]W. W. Ge, H. Liu, X. Y. Zhao, X. M. Pan, T. H. He, D. Lin, H. Q. Xu, and H. S. Luo, J. Alloys Compoun. **456**, 503 (2008).

[31]S. Trujillo, J. Kreisel, Q. Jiang, J. H. Smith, P. A. Thomas, P. Bouvier, and F. Weiss, J. Phys. Condens. Matter **17**, 6587 (2005).

[32]J. A. Sanjurjo, E. Lopezcruz, and G. Burns, Solid State Commun. **48**, 221 (1983).

[33]J. A. Sanjurjo, E. Lopezcruz, and G. Burns, Phys. Rev. B **28**, 7260 (1983).

[34]W. W. Ge, J. F. Li, D. Viehland, and H. S. Luo, J. Am. Ceram. Soc. **93**, 1372 (2010).

[35]R. Migoni, H. Bilz, and D. Bauerle, Phys. Rev. Lett. **37**, 1155 (1976).

[36]M. Elmarssi and H. Dammak, Solid State Commun. **142**, 487 (2007).

[37]K. Sakata and Y. Masuda, Ferroelectrics **7**, 347 (1974).

[38]L. E. Cross, Ferroelectrics **76**, 241 (1987).

[39]R. A. Cowley, Phys. Rev. B **134**, A981 (1964).

[40]Y. Fujii, S. Hoshino, Y. Yamada, and G. Shirane, Phys. Rev. B **9**, 4549 (1974).

[41]M. J. Haun, E. Furman, T. R. Halemane, and L. E. Cross, Ferroelectrics **99**, 55 (1989).

[42]X. H. Dai, Z. K. Xu, and D. Viehland, J. Am. Ceram. Soc. **78**, 2815 (1995).